- High length–diameter ratio nanotubes self-assembled from a facial cyclopeptide
  Qin, S.-Y.; Jiang, H.-F.; Liu, X.-J.; Pei, Y.; Cheng, H.; Sun, Y.-X.; Zhang, X.-Z. *Soft Matter* **2014**, *10,* 947-951.
  Abstract:

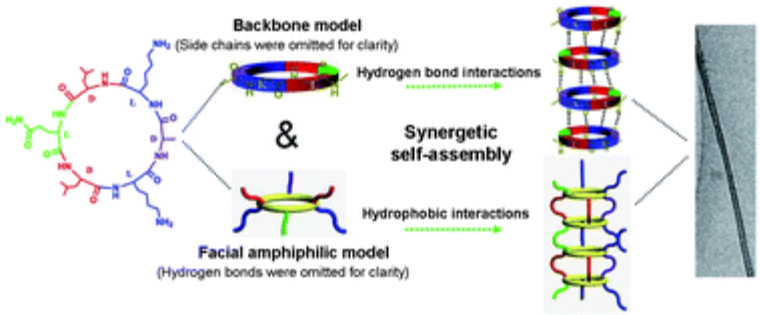

A six-residue facial cyclopeptide was designed with the following sequence: c-[D-Leu-L-Lys-D-Ala-L-Lys-D-Leu-L-Gln] (CP). Extensive hydrogen bonding between the cyclopeptide backbones mainly regulated CP to self-assemble into single-walled nanotubes. Simultaneously, the hydrophobic interaction among facial hydrophobic side chains of CP was introduced to stabilize the hydrogen bonding, resulting in the formation of the thick-walled nanotubes with high length–diameter ratios.

- Topochemical polymerization in self-assembled rodlike micelles of bisurea bolaamphiphiles
  Pal, A.; Voudouris, P.; Kenigs, M. M.; Besenius, P.; Wyss, H. M.; Degrmenci, V.; Sijbesma, R. P. *Soft Matter* **2014**, *10,* 952-956.
  Abstract:

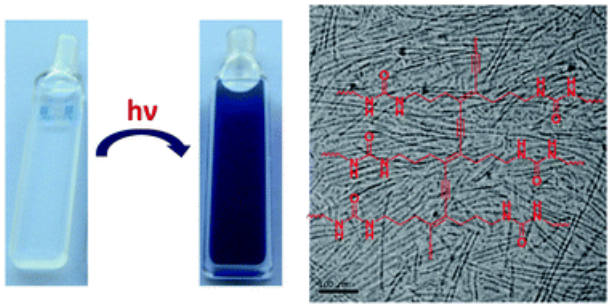

Rod-like micelles, formed from bolaamphiphiles with oligo(ethylene oxide) hydrophilic outer segments and a hydrophobic segment with diacetylene flanked by two urea moieties, were covalently fixated by topochemical photopolymerization to high degrees of polymerization by optimizing the hydrophobic core and the hydrophilic periphery of the bolaamphiphiles. Analysis of the polymerized product with dynamic light scattering in chloroform showed degrees of polymerization of approximately 250. Cryo-TEM of bolaamphiphiles before and after UV irradiation showed that the morphology of the rods was conserved upon topochemical polymerization.

- Hollow nanotubular toroidal polymer microrings
  Lee, J.; Baek, K.; Kim, M.; Yun, G.; Ko, Y. H.; Lee, N.-S.; Hwang, I.; Kim, J.; Natarajan, R.; Park, C. G.; Sung, W.; Kim, K. *Nature Chem.* **2014**, *6*, 97-103.
  Abstract:

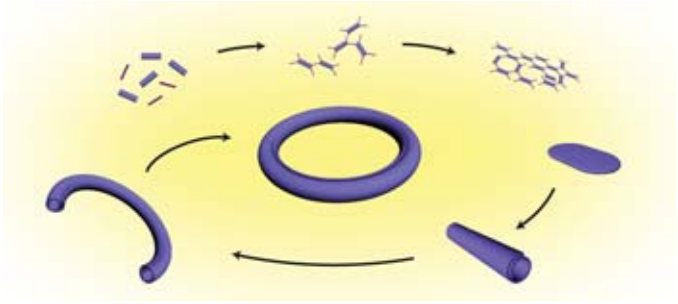

Mechanically robust and shape-persistent hollow toroidal polymer microrings have been synthesized directly by thiol-ene photopolymerization of rectangular-shaped monomers with dithiols. The size of the microrings can be tuned by varying the monomer concentration. The resulting structures can encapsulate molecules in their hollow interiors and also serve as scaffolds to template the formation of circular arrays of metal nanoparticles.

Despite the remarkable progress made in the self-assembly of nano- and microscale architectures with well-defined sizes and shapes, a self-organization-based synthesis of hollow toroids has, so far, proved to be elusive. Here, we report the synthesis of polymer microrings made from rectangular, flat and rigid-core monomers with anisotropically predisposed alkene groups, which are crosslinked with each other by dithiol linkers using thiol-ene photopolymerization. The resulting hollow toroidal structures are shape-persistent and mechanically robust in solution. In addition, their size can be tuned by controlling the initial monomer concentrations, an observation that is supported by a theoretical analysis. These hollow microrings can encapsulate guest molecules in the intratoroidal nanospace, and their peripheries can act as templates for circular arrays of metal nanoparticles.

- Synthesis of structurally well-defined and liquid-phase-processable graphene nanoribbons
  Narita, A.; Feng, X.; Hernandez, Y.; Jensen, S. A.; Bonn, M.; Yang, H.; Verzhbitskiy, I. A.; Casiraghi, C.; Hansen, M. R.; Koch, A. H. R.; Fytas, G.; Ivasenko, O.; Li, B.; Mali, K. S.; Balandina, T.; Mahesh, S.; De Feyter, S.; Müllen, K. *Nature Chem.* **2014**, *6*, 126-132.
  Abstract:

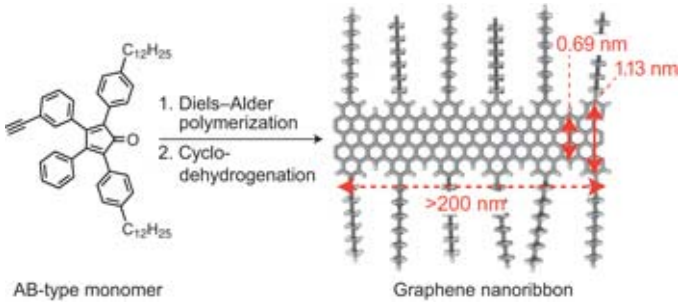

Liquid-phase-processable graphene nanoribbons (GNRs) over 200 nm long and with well-defined structures have now been synthesized by a bottom-up method, and are found to have a large optical bandgap of 1.88 eV. Scanning probe microscopy revealed highly ordered self-assembled monolayers of the GNRs, and the high intrinsic charge-carrier mobility of individual ribbons was characterized by terahertz spectroscopy.

The properties of graphene nanoribbons (GNRs) make them good candidates for next-generation electronic materials. Whereas ‘top-down’ methods, such as the lithographical patterning of graphene and the unzipping of carbon nanotubes, give mixtures of different GNRs, structurally well-defined GNRs can be made using a ‘bottom-up’ organic synthesis approach through solution-mediated or surface-assisted cyclodehydrogenation reactions. Specifically, non-planar polyphenylene precursors

were first 'built up' from small molecules, and then 'graphitized' and 'planarized' to yield GNRs. However, fabrication of processable and longitudinally well-extended GNRs has remained a major challenge. Here we report a bottom-up solution synthesis of long (>200 nm) liquid-phase-processable GNRs with a well-defined structure and a large optical bandgap of 1.88 eV. Self-assembled monolayers of GNRs can be observed by scanning probe microscopy, and non-contact time-resolved terahertz conductivity measurements reveal excellent charge-carrier mobility within individual GNRs. Such structurally well-defined GNRs may prove useful for fundamental studies of graphene nanostructures, as well as the development of GNR-based nanoelectronics.

- Nano-Imaging Feud Sets Online Sites Sizzling
  Service, R. F. *Science* **2014,** *343*, 358-358.
  Abstract:

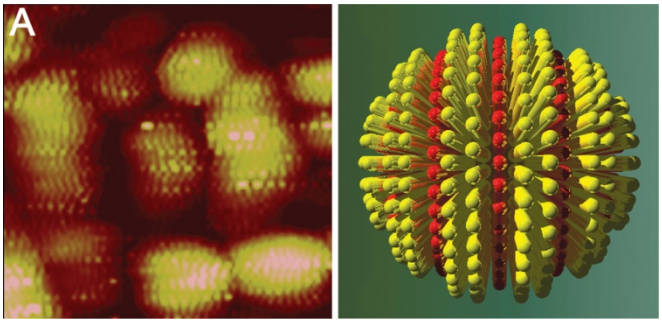

Scientific controversies often sort themselves out as new data roll in. But a decade-old dispute in nanoscience shows no sign of letting up. Researchers on both sides are claiming that recently published papers settle the debate in their favor, while one is charging his opponents with resorting to an electronic bullying campaign.

- Single-Crystal Linear Polymers Through Visible Light–Triggered Topochemical Quantitative Polymerization
  Dou, L.; Zheng, Y.; Shen, X.; Wu, G.; Fields, K.; Hsu, W.-C.; Zhou, H.; Yang, Y.; Wudl, F. *Science* **2014,** *343*, 272-277.
  Abstract:

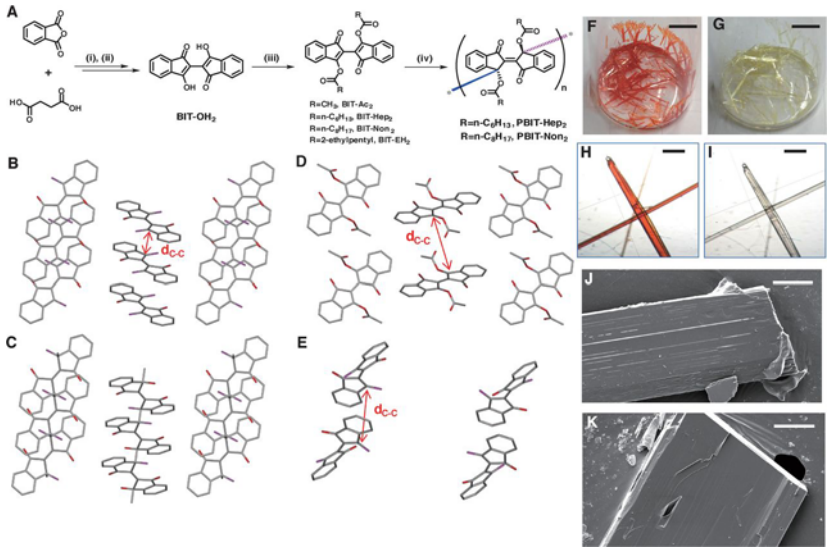

One of the challenges in polymer science has been to prepare large-polymer single crystals. We demonstrate a visible light–triggered quantitative topochemical polymerization reaction based on a

conjugated dye molecule. Macroscopic-size, high-quality polymer single crystals are obtained. Polymerization is not limited to single crystals, but can also be achieved in highly concentrated solution or semicrystalline thin films. In addition, we show that the polymer decomposes to monomer upon thermolysis, which indicates that the polymerization-depolymerization process is reversible. The physical properties of the polymer crystals enable us to isolate single-polymer strands via mechanical exfoliation, which makes it possible to study individual, long polymer chains.

- Many Paths to the Origin of Life
  Gollihar, J.; Levy, M.; Ellington, A. D. *Science* **2014,** *343*, 259-260.
  Abstract:

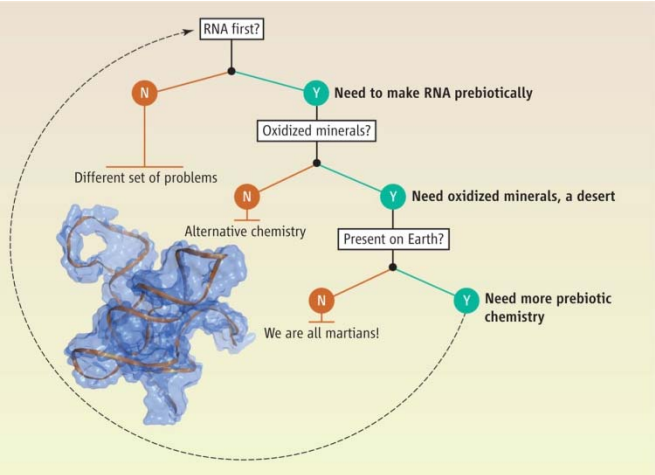

The origin of life remains a daunting mystery in part because rather than knowing too little, we increasingly know about too many possible mechanisms that might have led to the self-sustaining replication of nucleic acids and the cellularization of genetic material that is the basis of life on Earth.

- Transmissible Dog Cancer Genome Reveals the Origin and History of an Ancient Cell Lineage
  Murchison, E. P.; Wedge, D. C.; Alexandrov, L. B.; Fu, B.; Martincorena, I.; Ning, Z.; Tubio, J. M. C.; Werner, E. I.; Allen, J.; De Nardi, A. B.; Donelan, E. M.; Marino, G.; Fassati, A.; Campbell, P. J.; Yang, F.; Burt, A.; Weiss, R. A.; Stratton, M. R. *Science* **2014,** *343*, 437-440.
  Abstract:

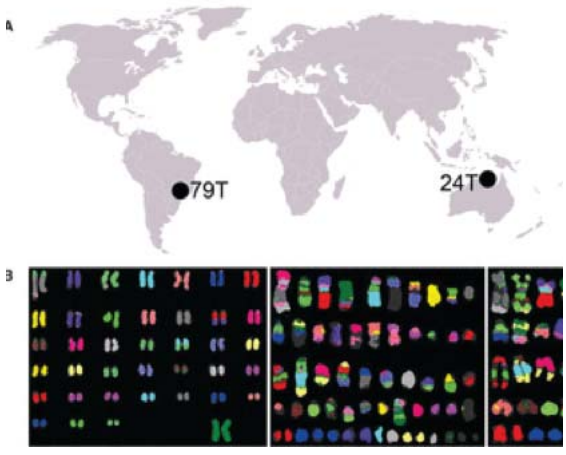

Canine transmissible venereal tumor (CTVT) is the oldest known somatic cell lineage. It is a transmissible cancer that propagates naturally in dogs. We sequenced the genomes of two CTVT tumors and found that CTVT has acquired 1.9 million somatic substitution mutations and bears

evidence of exposure to ultraviolet light. CTVT is remarkably stable and lacks subclonal heterogeneity despite thousands of rearrangements, copy-number changes, and retrotransposon insertions. More than 10,000 genes carry nonsynonymous variants, and 646 genes have been lost. CTVT first arose in a dog with low genomic heterozygosity that may have lived about 11,000 years ago. The cancer spawned by this individual dispersed across continents about 500 years ago. Our results provide a genetic identikit of an ancient dog and demonstrate the robustness of mammalian somatic cells to survive for millennia despite a massive mutation burden.

- Different Insight into Amphiphilic PEG-PLA Copolymers: Influence of Macromolecular Architecture on the Micelle Formation and Cellular Uptake
  Garofalo, C.; Capuano, G.; Sottile, R.; Tallerico, R.; Adami, R.; Reverchon, E.; Carbone, E.; Izzo, L.; Pappalardo, D. *Biomacromolecules* **2014**, *15*, 403–415.
  Abstract:

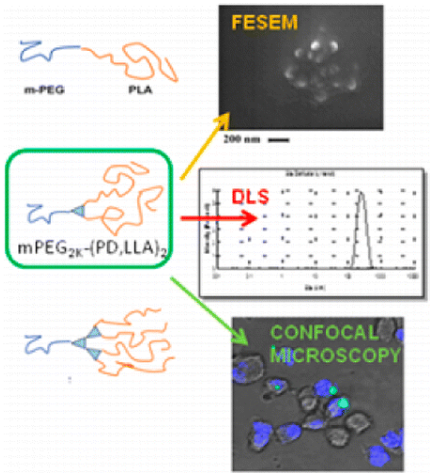

One constrain in the use of micellar carriers as drug delivery systems (DDSs) is their low stability in aqueous solution. In this study “tree-shaped” copolymers of general formula mPEG-$(PLA)_n$ (n = 1, 2 or 4; mPEG = poly(ethylene glycol) monomethylether 2K or 5K Da; PLA = atactic or isotactic poly(lactide)) were synthesized to evaluate the architecture and chemical composition effect on the micelles formation and stability. Copolymers with mPEG/PLA ratio of about 1:1 wt/wt were obtained using a “core-first” synthetic route. Dynamic Light Scattering (DLS), Field Emission Scanning Electron Microscopy (FESEM), and Zeta Potential measurements showed that $mPEG_{2K}$-$(PD,LLA)_2$ copolymer, characterized by mPEG chain of 2000 Da and two blocks of atactic PLA, was able to form monodisperse and stable micelles. To analyze the interaction among micelles and tumor cells, FITC conjugated mPEG-$(PLA)_n$ were synthesized. The derived micelles were tested on two, histological different, tumor cell lines: HEK293t and HeLa cells. Fluorescence Activated Cells Sorter (FACS) analysis showed that the FITC conjugated $mPEG_{2K}$-$(PD,LLA)_2$ copolymer stain tumor cells with high efficiency. Our data demonstrate that both PEG size and PLA structure control the biological interaction between the micelles and biological systems. Moreover, using confocal microscopy analysis, the staining of tumor cells obtained after incubation with $mPEG_{2K}$-$(PD,LLA)_2$ was shown to be localized inside the tumor cells. Indeed, the $mPEG_{2K}$-$(PD,LLA)_2$ paclitaxel-loaded micelles mediate a potent antitumor cytotoxicity effect.

- Conformational Distribution and α-Helix to β-Sheet Transition of Human Amylin Fragment Dimer

Qi, R.; Luo, Y.; Ma, B.; Nussinov, R.; Wei, G. *Biomacromolecules* **2014**, *15*, 122–131.

Abstract:

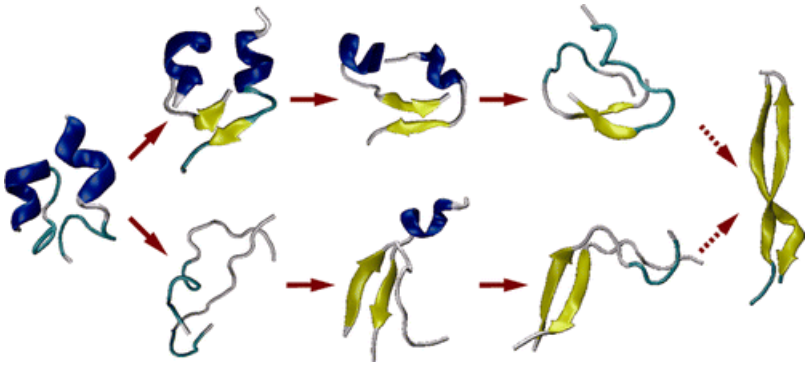

Experiments suggested that the fibrillation of the 11–25 fragment (hIAPP(11–25)) of human islet amyloid polypeptide (hIAPP or amylin) involves the formation of transient α-helical intermediates, followed by conversion to β-sheet-rich structure. However, atomic details of α-helical intermediates and the transition mechanism are mostly unknown. We investigated the structural properties of the monomer and dimer in atomistic detail by replica exchange molecular dynamics (REMD) simulations. Transient α-helical monomers and dimers were both observed in the REMD trajectories. Our calculated H^{α} chemical shifts based on the monomer REMD run are in agreement with the solution-state NMR experimental observations. Multiple 300 ns MD simulations at 310 K show that α-helix-to-β-sheet transition follows two mechanisms: the first involved direct transition of the random coil part of the helical conformation into antiparallel β-sheet, and in the second, the α-helical conformation unfolded and converted into antiparallel β-sheet. In both mechanisms, the α-helix-to-β-sheet transition occurred via random coil, and the transition was accompanied by an increase of interpeptide contacts. In addition, our REMD simulations revealed different temperature dependencies of helical and β-structures. Comparison with experimental data suggests that the propensity for hIAPP(11–25) to form α-helices and amyloid structures is concentration- and temperature-dependent.

- Hydrogen-Bond-Assisted Controlled C–H Functionalization via Adaptive Recognition of a Purine Directing Group

  Kim, H. J.; Ajitha, M. J.; Lee, Y.; Ryu, J.; Kim, J.; Lee, Y., Jung, Y.; Chang, S. *Am. Chem. Soc.* **2014,** *136*, 1132–1140.

  Abstract:

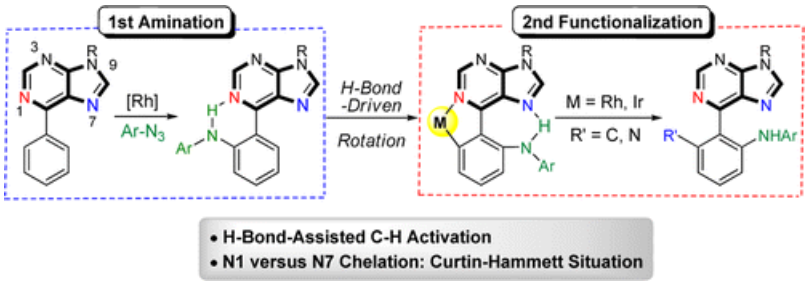

We have developed the Rh-catalyzed selective C–H functionalization of 6-arylpurines, in which the purine moiety directs the C–H bond activation of the aryl pendant. While the first C–H amination proceeds via the N1-chelation assistance, the subsequent second C–H bond activation takes advantage of an intramolecular hydrogen-bonding interaction between the initially formed amino group and one nitrogen atom, either N1 or N7, of the purinyl part. Isolation of a rhodacycle

intermediate and the substrate variation studies suggest that N1 is the main active site for the C–H functionalization of both the first and second amination in 6-arylpurines, while N7 plays an essential role in controlling the degree of functionalization serving as an intramolecular hydrogen-bonding site in the second amination process. This pseudo-Curtin–Hammett situation was supported by density functional calculations, which suggest that the intramolecular hydrogen-bonding capability helps second amination by reducing the steric repulsion between the first installed ArNH and the directing group.

- Reversible Photochemical Control of Singlet Oxygen Generation Using Diarylethene Photochromic Switches
  Hou, L.; Zhang, X.; Pijper, T. C.; Browne, W. R.; Feringa, B. L. *J. Am. Chem. Soc.* **2014**, *136*, 910-913.
  Abstract:

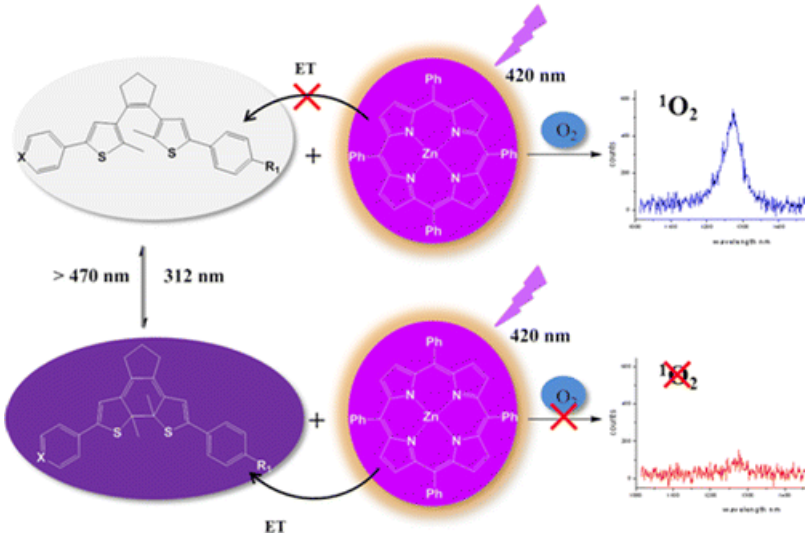

Reversible noninvasive control over the generation of singlet oxygen is demonstrated in a bicomponent system comprising a diarylethene photochromic switch and a porphyrin photosensitizer by selective irradiation at distinct wavelengths. The efficient generation of singlet oxygen by the photosensitizer is observed when the diarylethene unit is in the colorless open form. Singlet oxygen generation is not observed when the diarylethene is converted to the closed form. Irradiation of the closed form with visible light (>470 nm) leads to full recovery of the singlet oxygen generating ability of the porphyrin sensitizer.

- Enantioselective Component Selection in Multicomponent Supramolecular Gels
  Edwards, W.; Smith, D. K. *J. Am. Chem. Soc.* **2014**, *136*, 1116–1124.
  Abstract:

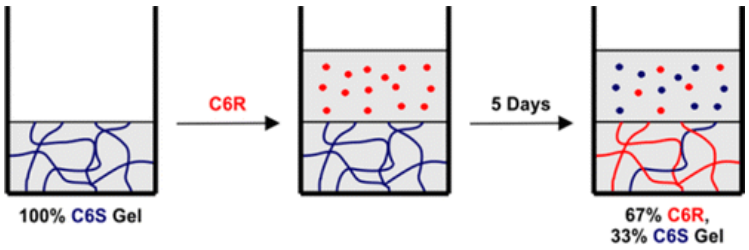

We investigate a two-component acid–amine gelation system in which chirality plays a vital role. A carboxylic acid based on a second generation l-lysine dendron interacts with chiral amines and

subsequently assembles into supramolecular gel fibers. The chirality of the amine controls the assembly of the resulting diastereomeric complexes, even if this chirality is relatively “poor quality”. Importantly, the selective incorporation of one enantiomer of an amine over the other into the gel network has been demonstrated, with the R amine that forms complexes which assemble into the most stable gel being primarily selected for incorporation. Thermodynamic control has been proven by forming a gel exclusively with an S amine, allowing the R enantiomer to diffuse through the gel network, and displacing it from the “solidlike” fibers, demonstrating that these gels adapt and evolve in response to chemical stimuli to which they are exposed. Excess amine, which remains unincorporated within the solidlike gel fiber network, can diffuse out and be reacted with an isocyanate, allowing us to quantify the enantioselectivity of component selection but also demonstrating how gels can act as selective reservoirs of potential reagents, releasing them on demand to undergo further reactions; hence, component-selective gel assembly can be coupled with controlled reactivity.

- Combinatorial Peptide Libraries: Mining for Cell-Binding Peptides
  Powell Gray, B.; Brown, K. C. *Chem. Rev.* **2014**, *114*, 1020–1081.
  Abstract:

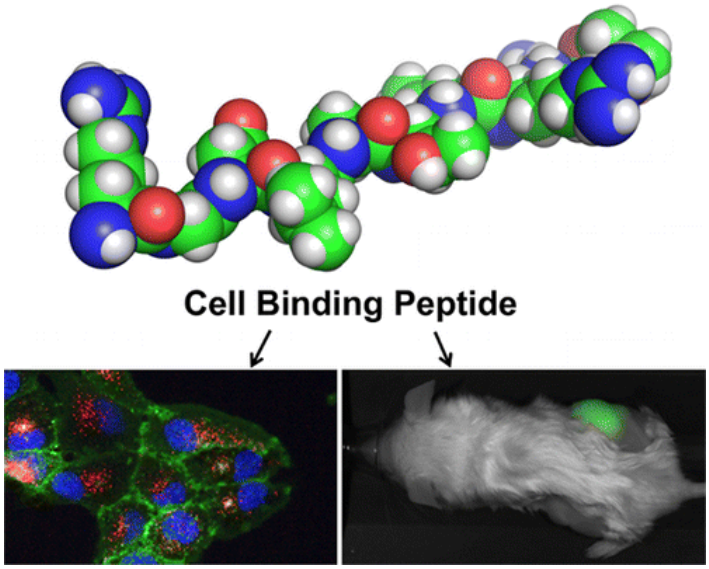

This review focuses on methods of selecting cell-targeting ligands from peptide libraries and the downstream use of these peptides. It includes the use of different types of peptide libraries and different selection methods. To highlight the utility of the selected ligands, we have not limited our discussion to a single cell type or disease state. Additionally, we have not merely concentrated on a single application in which these peptides can be used but have presented a broad overview of different applications. We focused on peptides isolated within the past five years but have also included peptides that have been widely used and merit discussion. It is our intention to present a complete compilation of cell-targeting peptides, but due to the scope of the field, we apologize if a peptide has been inadvertently missed. We have not included peptides that bind to nonmammalian cells, the use of naturally occurring peptide-targeting ligands, or studies using directed libraries based on known peptide sequences. Cell-penetrating peptides are not discussed as these peptides do not deliver cargo in a cell-specific fashion. These topics have been reviewed elsewhere.

- Design and Synthesis of Molecular Donors for Solution-Processed High-Efficiency Organic

Solar Cells

Coughlin, J. E.; Henson, Z. B.; Welch, G. C.; Bazan, G. C. *Acc. Chem. Res.* **2014**, *47*, 257–270.

Abstract:

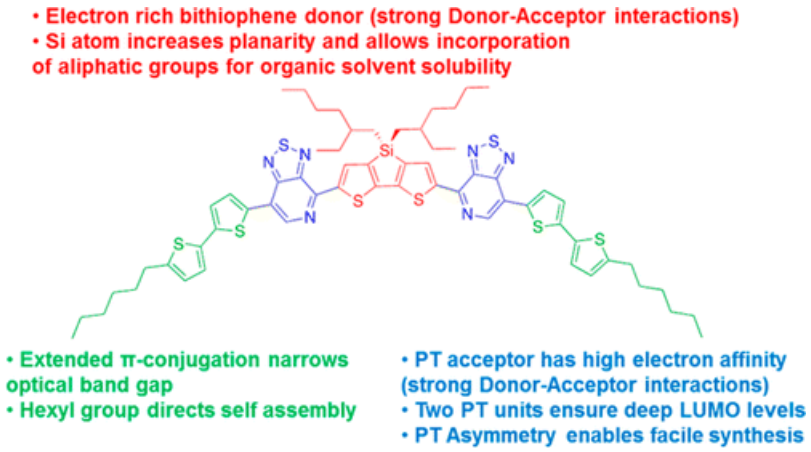

Organic semiconductors incorporated into solar cells using a bulk heterojunction (BHJ) construction show promise as a cleaner answer to increasing energy needs throughout the world. Organic solar cells based on the BHJ architecture have steadily increased in their device performance over the past two decades, with power conversion efficiencies reaching 10%. Much of this success has come with conjugated polymer/fullerene combinations, where optimized polymer design strategies, synthetic protocols, device fabrication procedures, and characterization methods have provided significant advancements in the technology. More recently, chemists have been paying particular attention to well-defined molecular donor systems due to their ease of functionalization, amenability to standard organic purification and characterization methods, and reduced batch-to-batch variability compared to polymer counterparts.

There are several critical properties for efficient small molecule donors. First, broad optical absorption needs to extend towards the near-IR region to achieve spectral overlap with the solar spectrum. Second, the low lying highest occupied molecular orbital (HOMO) energy levels need to be between −5.2 and −5.5 eV to ensure acceptable device open circuit voltages. Third, the structures need to be relatively planar to ensure close intermolecular contacts and high charge carrier mobilities. And last, the small molecule donors need to be sufficiently soluble in organic solvents (≥10 mg/mL) to facilitate solution deposition of thin films of appropriate uniformity and thickness. Ideally, these molecules should be constructed from cost-effective, sustainable building blocks using established, high yielding reactions in as few steps as possible. The structures should also be easy to functionalize to maximize tunability for desired properties.

In this Account, we present a chronological description of our thought process and design strategies used in the development of highly efficient molecular donors that achieve power conversion efficiencies greater than 7%. The molecules are based on a modular D^1-A-D^2-A-D^1architecture, where A is an asymmetric electron deficient heterocycle, which allowed us to quickly access a library of compounds and develop structure–property–performance relationships. Modifications to the D1 and D2 units enable spectral coverage throughout the entire visible region and control of HOMO energy levels, while adjustments to the pendant alkyl substituents dictate molecular solubility, thermal transition temperatures, and solid-state organizational tendencies. Additionally, we discuss regiochemical considerations that highlight how individual atom placements can significantly influence molecular and subsequently device characteristics.

Our results demonstrate the utility of this architecture for generating promising materials to be integrated into organic photovoltaic devices, call attention to areas for improvement, and provide guiding principles to sustain the steady increases necessary to move this technology forward.

- Modular Columnar Supramolecular Polymers as Scaffolds for Biomedical Applications
  Petkau-Milroy, K.; Sonntag, M. H.; Brunsveld, L., *Chem. Eur. J.* **2013**, *19*, 10786–10793.
  Abstract:

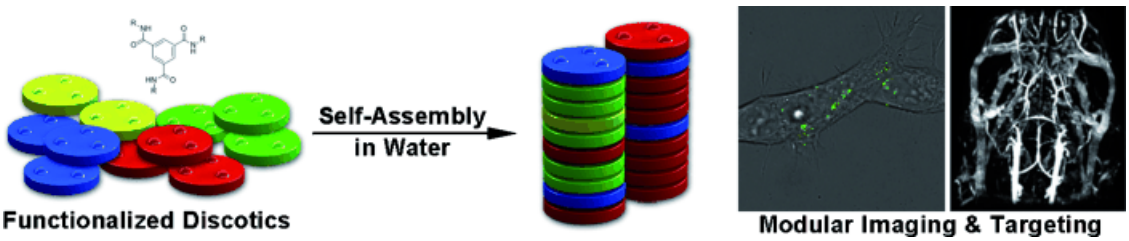

Self-assembly of discotic molecules into supramolecular polymers offers a flexible approach for the generation of multicomponent one-dimensional columnar architectures with tuneable biomedical properties. Decoration with ligands induces specific binding of the self-assembled scaffold to biological targets. The modular design allows the easy co-assembly of different discotics for the generation of probes for targeted imaging and cellular targeting with adjustable ligand density and composition.

- Supramolecular Polymers Based on Efficient Pillar[5]arene—Neutral Guest Motifs
  Li, C.; Han, K.; Li, J.; Zhang, Y.; Chen, W.; Yu, Y.; Jia, X., *Chem. Eur. J.* **2013**, *19*, 11892–11897.
  Abstract:

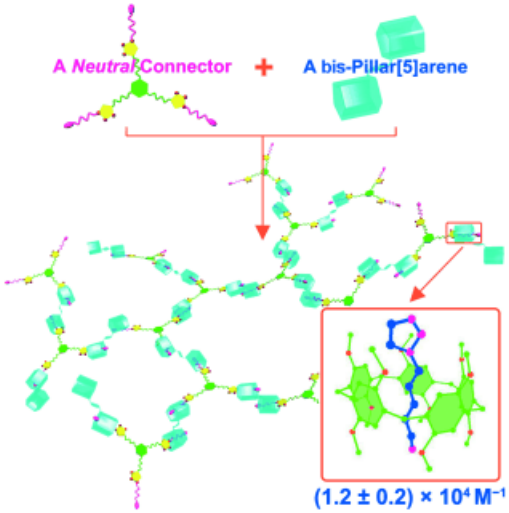

Neutral and efficient: A neutral guest with a cyano site and a triazole site, which can be easily prepared and modified, is demonstrated to strongly bind with pillar[5]arene (see figure). Based on this new recognition motif, two neutral supramolecular polymers in organic media, which are currently unfeasible by means of host–guest interactions of crown ethers and calixarenes, were fabricated. One is AA/BB-type, and the other is A_2/B_3-type.

- Processes To Separate Enantiomers
  Lorenz, H.; Seidel-Morgenstern, A. *Angew. Chem. Int. Ed*. **2014**, *53*, 1218–1250.
  Abstract:

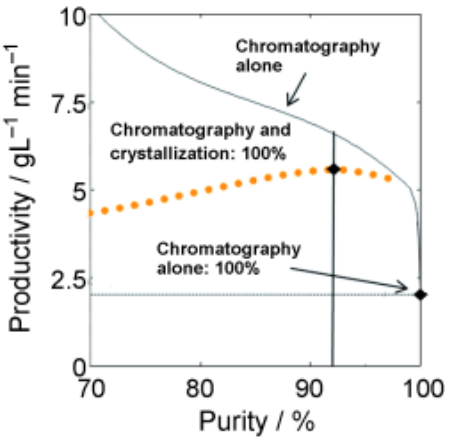

The provision of pure enantiomers is of increasing importance not only for the pharmaceutical industry but also for agrochemistry and biotechnology. In general, there are two rival approaches to provide pure enantiomers. The “chiral” approach is based on developing an asymmetric synthesis of just one of the enantiomers, while the “racemic” approach is based on separating mixtures of the two enantiomers. In the last few years remarkable progress has been achieved in the latter area. This Review focuses in particular on enantioselective crystallization processes and preparative chromatography, including hybrid processes and the incorporation of racemization steps. Several examples from our research are used for illustration purposes.

- Through-Bond/Through-Space Anion Relay Chemistry Exploiting Vinylepoxides as Bifunctional Linchpins
  Chen, M. Z.; Gutierrez, O.; Smith, A. B. *Angew. Chem. Int. Ed*. **2014** *53*, 1279–1282.
  Abstract:

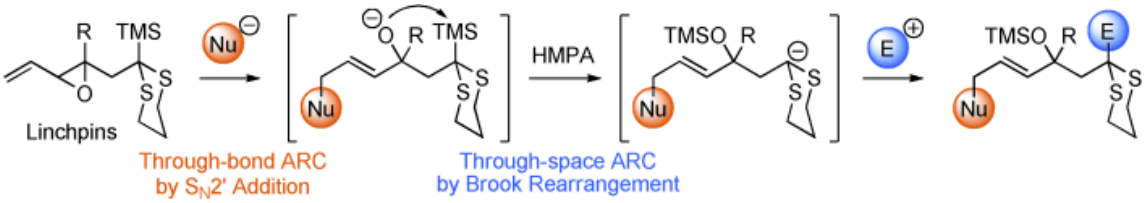

The development of new bifunctional linchpins that permit the union of diverse building blocks is essential for the synthetic utility of anion relay chemistry (ARC). The design, synthesis, and validation of three vinylepoxide linchpins for through-bond/through-space ARC are now reported. For negative charge migration, this class of bifunctional linchpins employs initial through-bond ARC by an S_N2' reaction, followed by through-space ARC exploiting a 1,4-Brook rearrangement. The *trans*-disubstituted vinylepoxide linchpin yields a mixture of *E*/*Z* isomers, whereas the *cis*-disubstituted and the *trans*-trisubstituted vinylepoxide linchpins proceed to deliver three-component adducts with excellent *E* selectivity.

- Structure and Ultrasonic Sensitivity of the Superparticles Formed by Self-Assembly of Single Chain Janus Nanoparticles
  Zhou, F.; Xie, M.; Chen, D. *Macromolecules* **2014**, *47*, 365–372.
  Abstract:

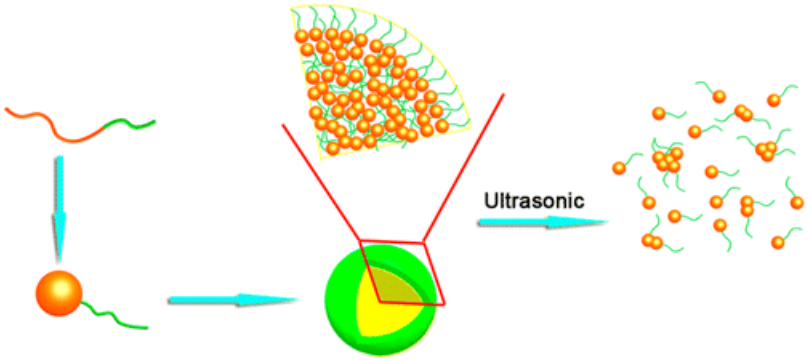

Single chain Janus nanoparticles (SCJNPs) (tadpole-like Janus nanoparticles) with a PEO (poly(ethylene oxide)) chain as the "tail" and a cross-linked PCEMA (poly(2-cinnamoyloxyethyl methacrylate)) chain as the "head" were synthesized conveniently and efficiently by directly photo-cross-linking PCEMA block of PEO-b-PCEMA diblock copolymer in the common solvent DMF; intramolecular cross-linking occurred dominantly at a relatively high concentration of the copolymer when the cross-linking speed is relatively low, leading to SCJNPs. In selective solvent for the "tails", the rigid "heads" aggregated into superparticles. It is significant that under a gentle ultrasonic treatment (40 kHz for 10 min) the spherical superparticles formed in DMF/ethanol (1/4, v/v) dissociated into individual SCJNPs. It is also demonstrated that even in pure water in which the superparticles have a more closely aggregated structure, there are still hydrophilic channels within the superparticles connecting the surrounding medium and the inside of the superparticles, which allows rapid transport of hydrophilic small molecules within the superparticles, as demonstrated by the fast acid quench of fluorescence of the encapsulated ANS (8-anilino-1-naphthalenesulfonate). These features should make the superparticles promising in the applications as templates for biomimetic mineralization, highly efficient microreactors for interfacial chemical reactions, and ultrasound responsive nanovehicles for controlled drug release.

- Interfacial Phenomena of Solvent-Diluted Block Copolymers
  Cohen, S.; Andelman, D. *Macromolecules* **2014**, *47*, 460–469.
  Abstract:

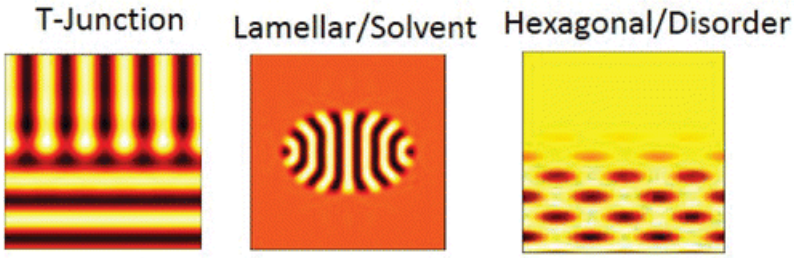

A phenomenological mean-field theory is used to investigate the properties of solvent-diluted diblock copolymers (BCP), in which the two BCP components (A and B) form a variety of phases that are diluted by a solvent (S). Using this approach, we model mixtures of diblock copolymers and a solvent and obtained the corresponding critical behavior. In the low solvent limit, we find how the critical point depends on the solvent density. Because of the nonlinear nature of the coupling between the A/B and BCP/solvent concentrations, the A/B modulation induces modulations in the polymer–solvent relative concentration with a double wavenumber. The free boundary separating the polymer-rich phase from the solvent-rich one is studied in two situations. First, we show how the presence of a chemically patterned substrate leads to deformations of the BCP film/solvent interface, creation of terraces in lamellar BCP film and even formation of multidomain droplets as induced by

the patterned substrate. Our results are in agreement with previous self-consistent field theory calculations. Second, we compare the surface tension between parallel lamellae coexisting with a solvent phase with that of a perpendicular one, and show that the surface tension has a nonmonotonic dependence on temperature. The anisotropic surface tension can lead to deformation of spherical BCP droplets into lens-shaped ones, together with reorientation of the lamellae inside the droplet during the polymer/solvent phase separation process in agreement with experiment.

- π-Conjugated Molecules Crosslinked Graphene-Based Ultrathin Films and Their Tunable Performances in Organic Nanoelectronics
  Ou, X.; Chen, P.; Jiang, L.; Shen, Y.; Hu, W.; Liu, M. *Adv. Func. Mater*. **2014**, *24*, 543-554.
  Abstract:

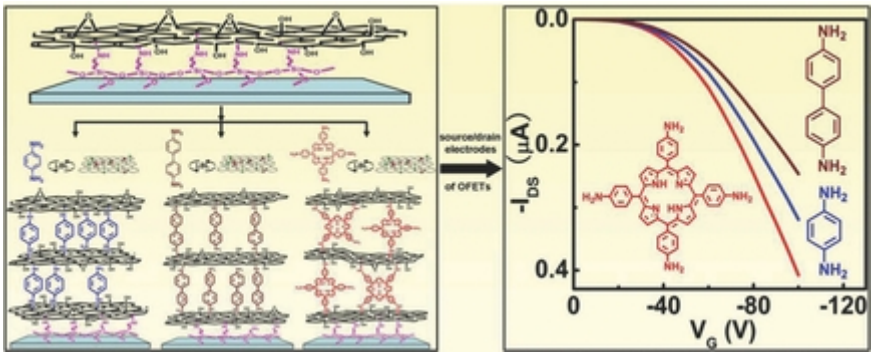

Graphene-based ultrathin films simultaneously featured with tunable performance, controlled thickness, and high stability, are integrated using π-conjugated molecules as cross-linkages. The use of dual functional linkage endows our new protocol with broad opportunities for desired motives in terms of using elaborately-designed linkages of desired functions.

- Polymer-Based Resistive Memory Materials and Devices
  Lin, W.; Liu, S.; Gong, T.; Zhao, Q.; Huang, W. *Adv. Mater*. **2014**, *26*, 570-606.
  Abstract :

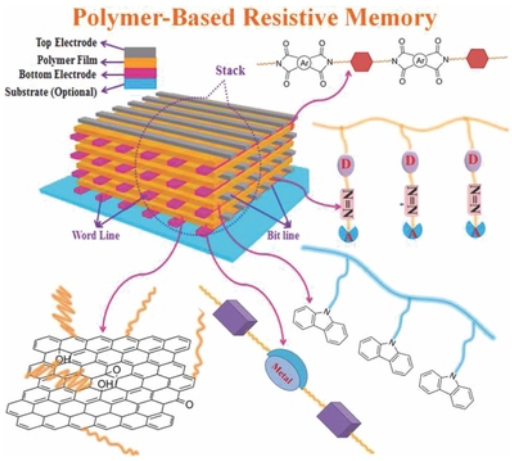

In this review we introduce the general characteristics of the device structures and fabrication, memory effects, and switching mechanisms of polymer-based resistive memory devices. Subsequently, the research progress concerning the use of single polymers or polymer composites as active materials for resistive memory devices are summarized. Finally, current challenges and future research directions in this field are discussed.

- Metal-driven hierarchical self-assembled zigzag nanoarchitectures with electrical conductivity
  Qiao, Y.; Lin, Y.; Liu, S.; Zhang, S.; Chen, H.; Wang, Y.; Yan, Y.; Guo, X.; Huang, J. *Chem. Commun.* **2014***, 49,* 704-706.
  Abstract:

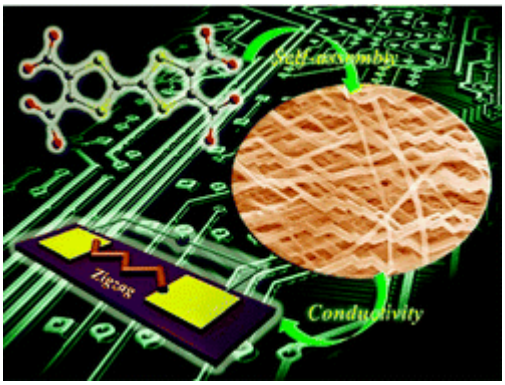

Quasi-one-dimensional electroactive materials with zigzag shape are fabricated by supramolecular self-assembly of a tetrathiafulvalene (TTF) derivative and metal ions under mild conditions. This is the first time that self-assembled organic conductors with zigzag shape are reported.

- A water soluble probe with near infrared two-photon absorption and polarity-induced fluorescence for cerebral vascular imaging
  Massin, J.; Charaf-Eddin, A.; Appaix, F.; Bretonniere, Y.; Jacquemin, D.; van der Sanden, B.; Monnereau, C.; Andraud, C. *Chem. Sci.* **2014***, 4*, 2833-2843.
  Abstract:

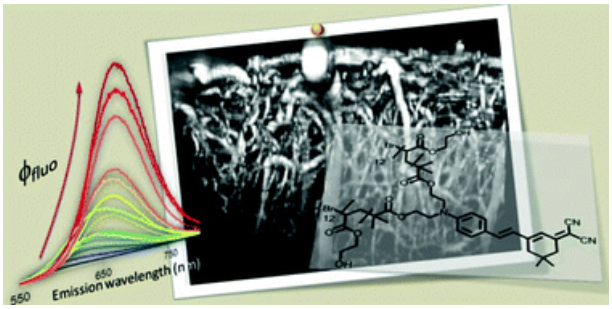

A water soluble Lemke chromophore derivative shows an unusual polarity dependence of its emission efficiency, leading to strong red-NIR fluorescence in water when fitted with appropriate water-solubilizing polymer chains. In this edge article, the synthesis of the chromophore is described. The dependence of its fluorescence on solvent polarity is investigated experimentally and rationalized on the basis of *ab initio* calculations. Finally, we demonstrate that this chromophore is a valuable candidate for *in vivo* two-photon imaging of cerebral vasculature, with two-photon absorption and emission in the biological transparency window.

- Skeletal Recombination Reaction of N-Fused Pentaphyrin (1.1.1.1.1) via Bromination
  Suzuki, M.; Hoshino, T.; Neya, S. *Org. Lett.* **2014,** *16*, 327-329.
  Abstract:

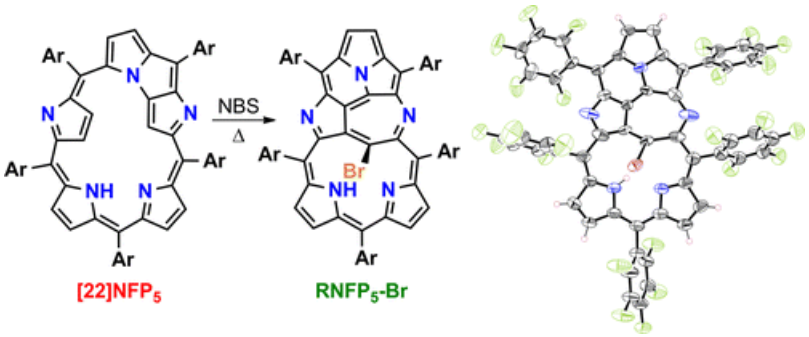

N-Fused [22] pentaphyrin(1.1.1.1.1) transformed into recombined *N*-fused pentaphyrin bromide after treatment with *N*-bromosuccinimide. This bromide was highly reactive to nucleophiles to give the corresponding substituted products including aminated, oxidized, and unsubstituted derivatives.

- Myristicyclins A and B: Antimalarial Procyanidins from Horsfieldia spicata from Papua New Guinea
  Lu, Z.; Van Wagoner, R. M.; Pond, C. D.; Pole, A. R.; Jensen, J. B.; Blankenship, D. A.; Grimberg, B. T.; Kiapranis, R.; Matainaho, T. K.; Barrows, L. R.; Ireland, C. M. *Org. Lett.* **2014,** *16*, 346-349.
  Abstract:

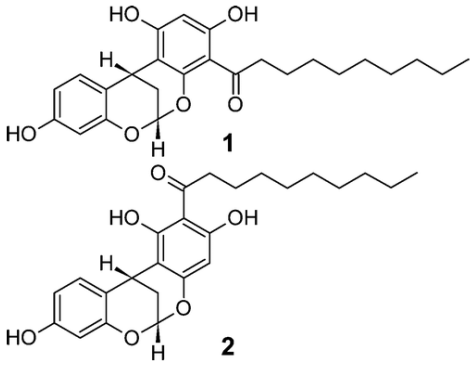

An antimalarial screen for plants collected from Papua New Guinea identified an extract of *Horsfieldia spicata* as having activity. Isolation of the active constituents led to the identification of two new compounds: myristicyclins A (**1**) and B (**2**). Both compounds are procyanidin-like congeners of myristinins lacking a pendant aromatic ring. Myristicyclin A was found to inhibit the ring, trophozoite, and schizont stages of *Plasmodium falciparum* at similar concentrations in the mid-µM range.

- Preparation of solid silver nanoparticles for inkjet printed flexible electronics with high conductivity
  Shen, W.; Zhang, X.; Huang, Q.; Xu, Q.; Song, W. *Nanoscale* **2014**, *6*, 1622–1628.
  Abstract:

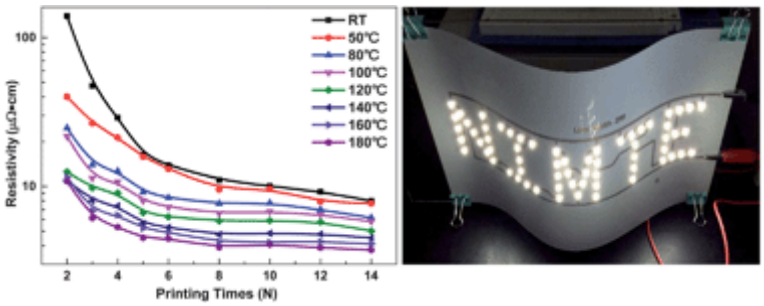

Silver nanoparticles (NPs) which could be kept in solid form and were easily stored without degeneration or oxidation at room temperature for a long period of time were synthesized by a simple and environmentally friendly wet chemistry method in an aqueous phase. Highly stable dispersions of aqueous silver NP inks, sintered at room temperature, for printing highly conductive tracks ([similar]8.0 μΩ cm) were prepared simply by dispersing the synthesized silver NP powder in water. These inks are stable, fairly homogeneous and suitable for a wide range of patterning techniques. The inks were successfully printed on paper and polyethylene terephthalate (PET) substrates using a common color printer. Upon annealing at 180 °C, the resistivity of the printed silver patterns decreased to 3.7 μΩ cm, which is close to twice that of bulk silver. Various factors affecting the resistivity of the printed silver patterns, such as annealing temperature and the number of printing cycles, were investigated. The resulting high conductivity of the printed silver patterns reached over 20% of the bulk silver value under ambient conditions, which enabled the fabrication of flexible electronic devices, as demonstrated by the inkjet printing of conductive circuits of LED devices.

- Color-Switchable Electroluminescence of Carbon Dot Light-Emitting Diodes
  Zhang, X.; Zhang, Y.; Wang, Y.; Kalytchuk, S.; Kershaw, S. V.; Wang, Y.; Wang, P.; Zhang, T.; Zhao, Y.; Zhang, H.; Cui, T.; Wang, Y.; Zhao, J.; Yu, W. W.; Rogach, A. L. *ACS Nano* **2013**, *7*, 11234–11241.
  Abstract:

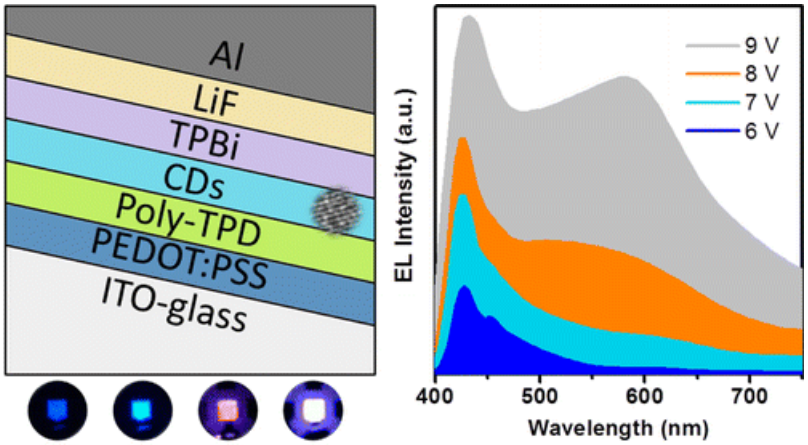

Carbon-dot based light-emitting diodes (LEDs) with driving current controlled color change are reported. These devices consist of a carbon-dot emissive layer sandwiched between an organic hole transport layer and an organic or inorganic electron transport layer fabricated by a solution-based process. By tuning the device structure and the injecting current density (by changing the applied voltage), we can obtain multicolor emission of blue, cyan, magenta, and white from the same carbon dots. Such a switchable EL behavior with white emission has not been observed thus far in single emitting layer structured nanomaterial LEDs. This interesting current density-dependent emission is useful for the development of colorful LEDs. The pure blue and white emissions are obtained by tuning the electron transport layer materials and the thickness of electrode.

- Assembly of an Injectable Noncytotoxic Peptide-Based Hydrogelator for Sustained Release of Drugs
  Baral, A.; Roy, S.; Hamley, I. W.; Mohapatra, S.; Ghosh, S.; Banerjee, A. *Langmuir* **2014**, *3*, 929–936.

Abstract:

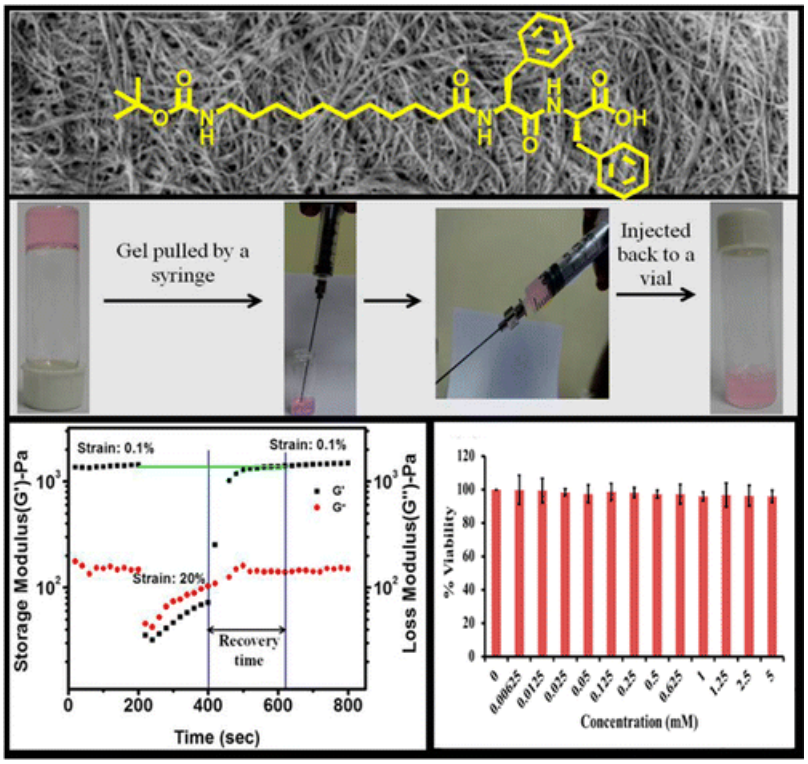

A new synthetic tripeptide-based hydrogel has been discovered at physiological pH and temperature. This hydrogel has been thoroughly characterized using different techniques including field emission scanning electron microscopic (FE-SEM) and high-resolution transmission electron microscopic (HR-TEM) imaging, small- and wide-angle X-ray diffraction analyses, FT-IR, circular dichroism, and rheometric analyses. Moreover, this gel exhibits thixotropy and injectability. This hydrogel has been used for entrapment and sustained release of an antibiotic vancomycin and vitamin B_{12} at physiological pH and temperature for about 2 days. Interestingly, MTT assay of these gelator molecules shows almost 100% cell viability of this peptide gelator, indicating its noncytotoxicity.

- Ultrathin Gold Nanoribbons Synthesized within the Interior Cavity of a Self-Assembled Peptide Nanoarchitecture
  Tomikazi, K.-Y.; Wakizaka, S.; Yamaguchi, Y.; Kobayashi, A.; Imai, T. *Langmuir* **2014**, *3*, 846–856.
  Abstract:

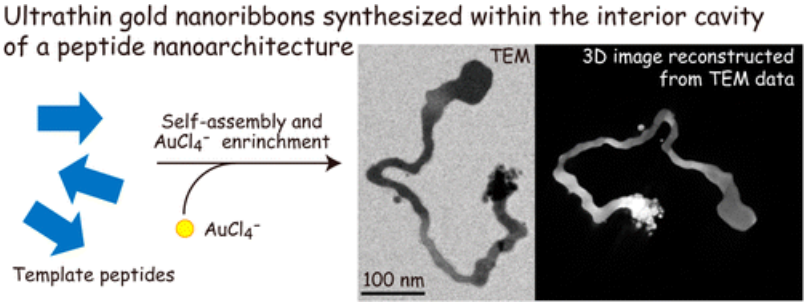

There is increasing interest in gold nanocrystals due to their unique physical, chemical, and biocompatible properties. In order to develop a template-assisted method for the fabrication of gold nanocrystals, we demonstrate here the *de novo* design and synthesis of a β-sheet-forming nonapeptide (RU006: Ac-AIAKAXKIA-NH_2, X = l-2-naphthylalanine) which undergoes self-assembly to

form disk-like nanoarchitectures approximately 100 nm wide and 2.5 nm high. These self-assemblies tend to form a network of higher-order assemblies in ultrapure water. Using RU006 as a template molecule, we fabricated ultrathin gold nanoribbons 50–100 nm wide, 2.5 nm high, and micrometers long without external reductants. Furthermore, in order to determine the mechanism of ultrathin gold nanoribbon formation, we synthesized four different RU006 analogues. On the basis of the results obtained using RU006 and these analogues, we propose the following mechanism for the self-assembly of RU006. First, RU006 forms a network by the cooperative association of disk-like assemblies in the presence of $AuCl_4^-$ ions that are encapsulated and concentrated within the interior cavity of the network architectures. This is followed by electron transfer from the naphthalene rings to Au^{III}, resulting in slow growth to form ultrathin gold nanoribbons along the template network architectures under ambient conditions. The resulting ribbons retain the dimensions of the cavity of the template architecture. Our approach will allow the construction of diverse template architectural morphologies and will find applications in the construction of a variety of metallic nanoarchitectures.

- Novel dibenzo[a,e]pentalene-based conjugated polymers
  Nakano, M.; Osaka, I.; Takimiya, K.; Koganezawac, T. *J. Mater. Chem. C* **2014**, *2*, 64–70.
  Abstract:

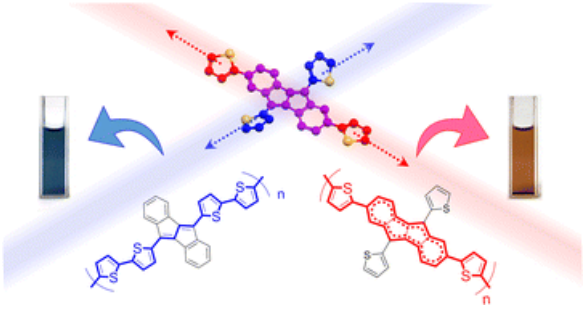

Dibenzo[a,e]pentalene (DBP), a ladder-type fused-ring system with 16π anti-aromatic nature, is integrated into conjugated polymers with oligothiophene building blocks to examine the potential of DBP as a new building block for semiconducting polymers. Depending on the incorporation manner of the DBP unit in the polymer backbone, via the 5,10- or 2,7-positions, the polymers show distinct colours, reflecting the different electronic structures, though the HOMO and LUMO energy levels estimated from cyclic voltammograms are almost the same. Interestingly, the impact of the incorporation manner was observed in the characteristics of their field-effect transistors (FETs). For PDTDBP2Ts, in which the DBP units are integrated into the polymer backbone via the 5,10-positions, the DBP units behave like a “dibenzo-annulated 1,3-butadiene” moiety, and their FET characteristics are strongly affected by orientational ordering and crystallinity, similar to ordinary “donor-only” polymers such as P3HT. On the other hand, iPDTDBP2Ts, in which the whole 16π DBP unit is integrated into the polymer backbone via the 2,7-positions, behave like a certain kind of donor-acceptor polymers, and the FET characteristics are independent of orientational order: the field-effect mobilities are higher than 0.1 cm2 V−1 s−1 regardless of the polymer orientation in the thin film. From these results, we can recognize the 16π anti-aromatic DBP unit as a useful building block with transmutable nature for the development of new conjugated polymers.

- High-efficiency deep-blue organic light-emitting diodes based on a thermally activated delayed fluorescence emitter
  Wu, S.; Aonuma, M.; Zhang, Q.; Huang, S.; Nakagawa, T.; Kuwabaraa, K.; Adachi, C. *J. Mater.*

Chem. C **2014**, *2*, 421–424.

Abstract:

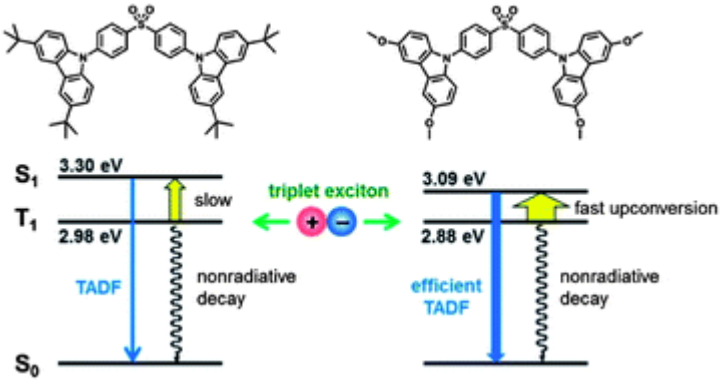

Highly efficient deep-blue thermally activated delayed fluorescence (TADF) is observed from a charge-transfer compound bis[4-(3,6-dimethoxycarbazole)phenyl]sulfone (DMOC-DPS). In comparison with the previously reported carbazole/sulfone derivative with tert-butyl substituents on the carbazole donors, DMOC-DPS exhibits a much shorter excited-state lifetime in both an aromatic solution and an organic thin film, because the change of the substituent on the donor affects the molecular energy levels of the first singlet (S1) and triplet (T1) excited states in different ways, decreasing the energy gap between S1 and T1 (ΔEST). An organic light emitting diode (OLED) based on DMOC-DPS achieves a maximum external electroluminescence quantum efficiency (EQE) of 14.5% and reduced efficiency roll-off, with Commission Internationale de L'Eclairage (CIE) coordinates of (0.16, 0.16), owing to efficient exciton harvesting that occurs through triplet-to-singlet up-conversion.